Radiation Physics and Chemistry 166 (2020) 108450

Contents lists available at ScienceDirect

Radiation Physics and Chemistry

journal homepage: www.elsevier.com/locate/radphyschem

On the physical, chemical, and neutron shielding properties of polyethylene/boron carbide composites

Zaheer Uddin[a], Tariq Yasin[b], Muhammad Shafiq[b,*], Asif Raza[c], Awais Zahur[d]

[a] Department of Metallurgy and Materials Engineering, Pakistan Institute of Engineering & Applied Sciences, Nilore, Islamabad, 45650, Pakistan
[b] Department of Chemistry, Pakistan Institute of Engineering & Applied Sciences, Nilore, Islamabad, 45650, Pakistan
[c] Department of Chemical Engineering, Pakistan Institute of Engineering & Applied Sciences, Nilore, Islamabad, 45650, Pakistan
[d] Department of Nuclear Engineering, Pakistan Institute of Engineering & Applied Sciences, Nilore, Islamabad, 45650, Pakistan

ARTICLE INFO

Keywords:
Neutron shielding
Polymer composite
Boron carbide
Fast neutrons
Monte Carlo simulation
Borated polyethylene

ABSTRACT

Monte Carlo methods are used for solving difficult stochastic problems in radiation shielding applications. The aim of this paper is to show the possibility of using the Monte Carlo code (MCBEND®) for evaluation and optimization of polyethylene with high boron loadings (for up to 40%) to reach better neutron shielding against fast neutrons (Am-Be neutron source). Boron is incorporated in polyethylene as boron carbide (B_4C). MCBEND® (Monte Carlo code developed by ANSWERS) is used to simulate neutron transport through the developed borated polyethylene composites. In order to verify the computer simulations, neutron detection and data acquisition systems have been assembled, modified, and thoroughly tested for shielding efficiency. It is shown that borated composite with 10% of boron content showed the highest experimental mass removal cross section. Moreover, composite formulation with 10% of boron shows optimum density, morphology, mechanical attributes, and thermal stability than that of the neat polyethylene matrix. A comparison of experimental and simulation mass removal cross sections shows that the geometry and physics models proposed in this work are in close agreement, with maximum relative difference of not more than 15%.

1. Introduction

Modern world finds extensive utilization of radiations, radioisotopes, and energy-related materials in power generation, medicine, and aerospace sectors. Neutrons are an important class of nuclear radiations, which do not possess net electric charge; therefore they cannot be stopped by electric forces. Neutron shielding is based on the principle of attenuation, which is an ability to mitigate the radiation effects by blocking or bouncing through a barrier material. Neutrons can be rendered less harmful through elastic and inelastic scattering (John and Lamarsh, 1955; Martin, 2013; Murray, 2014). Fast reactors typically involve high energy neutrons that must be shielded for efficient operation. Since fast reactors do not require moderation, shield design must include materials containing high hydrogen content to ensure thermalization followed by the absorption of fast neutrons. Hydrogen and hydrogen-based materials are preferred for moderating fast neutrons most probably by forming cross-sections that may interact with these neutrons. Compounds with a higher content of hydrogen, such as polyethylene (PE), paraffin wax (PW), and water form efficient neutron barriers. Moreover, neutron shielding properties may be further improved by incorporating boron salts (Abd and Elkady, 2014; Groves, 2017; Uhlář et al., 2013).

Monte Carlo methods physically simulate the fate of individual particle (neutron) and help predict detailed radiation level in a geometrical system. The possible outcome is some form of radiation dose, radiation damage, or an instrumental response to a particular radiation. These simulations find diverse applications in reactor operation, nuclear fuel management, incident detection systems, and personal dose uptake. With advances in the field of composites, new materials are being developed, evaluated, and applied for radiation shielding applications (Geoff et al., 2017; Kyrieleis, 2014).

Polymer composites have been widely used for radiation shielding applications because of their light weight, easy process-ability, and chemical inertness. Moreover, these materials can be easily incorporated with boron containing salts to further influence radiation shielding phenomenon. Consequently, borated polymer composites possessed good physico-mechanical properties than that of their neat counterparts and many researchers have investigated the use of such

Abbreviations: Boron carbide, B_4C; Am-Be, Americium–Beryllium

* Corresponding author.
E-mail address: shafiq@pieas.edu.pk (M. Shafiq).

https://doi.org/10.1016/j.radphyschem.2019.108450
Received 1 November 2018; Received in revised form 18 July 2019; Accepted 11 August 2019
Available online 13 August 2019
0969-806X/

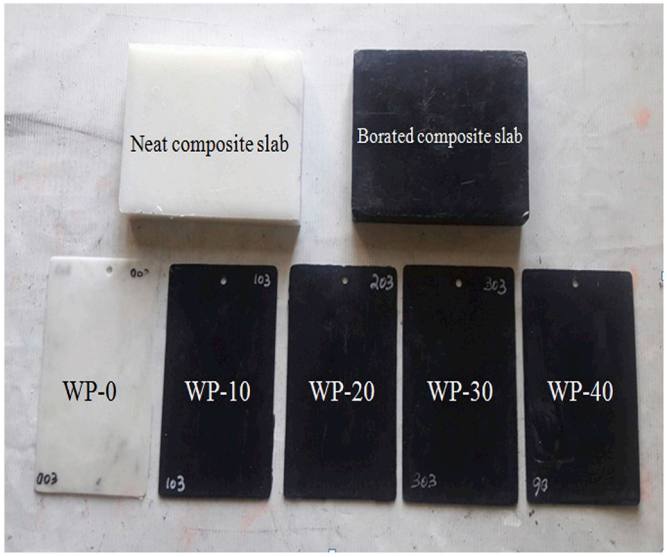

Fig. 1. Neat and borated composite formulations.

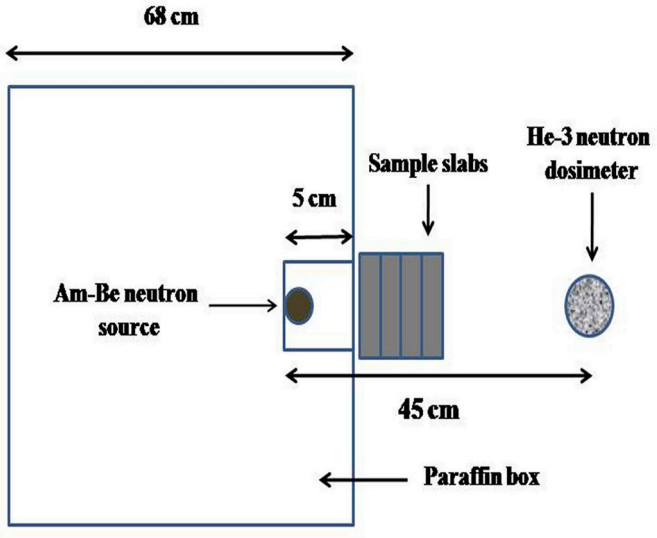

Fig. 2. Schematic diagram of experimental/simulation setup used for neutron shielding measurements.

polymer composites for radiation shielding applications (Akay, 2006; Shackelford and Alexander, 2000; Sperling, 2006a).

In previous studies, PE composites containing boron carbide (B_4C) showed good neutron and proton shielding properties (Harrison et al., 2008b). Paraffin with different loadings of oil has also been investigated as a neutron moderator and shield for Am-Be source (Aygün and Budak, 2012). High density polyethylene (HDPE) composites containing B_4C were developed for thermal neutron shielding applications. HDPE/B_4C composites with 24 phr (parts per hundred) of B_4C showed excellent shielding against thermal neutrons (Yasin and Khan, 2008).

The aim of this study is to evaluate the effect of higher boron content (for up to 40%) on the physico-chemical and fast neutron shielding properties of HDPE composites. Hybrids containing HDPE and PW served as polymer matrices and B_4C acted as reinforcement. PW was incorporated into polymer blends due to the presence of higher hydrogen content to influence neutron shielding. The effects of such high boron content on physical, thermal, mechanical, and neutron shielding properties of developed composites were investigated. Experimental neutron shielding measurements were compared with MCBEND® simulation results.

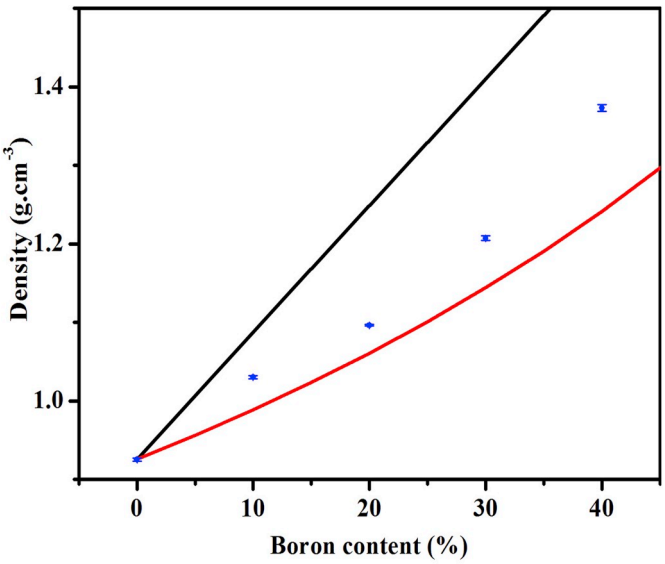

Fig. 3. FTIR spectra of pure HDPE and HDPE/B_4C composite.

2. Experimental

2.1. Materials

The main ingredients were soft paraffin wax (product code: 411663, Sigma Aldrich, USA, m.p ~ 65 °C), HDPE (product code: M20056, SABIC, Saudi Arabia, MFI ~ 20 g.10 min^{-1}, ρ = 0.956 g cm^{-3}), B_4C (Dunhua Zhengxing Abrasives Co. Ltd. China, ρ = 2.52 g cm^{-3}), stearic acid (Sigma-Aldrich), Irganox 1076 (Ciba Inc.), and irgafos 168 (Ciba Inc.).

2.2. Fabrication of composites

PW was first blended with B_4C at 80 °C in a glass beaker on a hot plate. It was then mixed with HDPE in an internal mixer (thermo

Table 1
Composition of five distinct HDPE/B_4C composites.

Formulation Code	HDPE (%)	PW (%)	B_4C (%)	Stearic acid (%)	Irganox 1076 (%)	Irgafos 168 (%)	^{Natural} B (%)
WP-0	49.45	49.45	0.00	0.95	0.10	0.05	0.00
WP-10	43.00	43.00	12.91	0.95	0.10	0.05	10.0
WP-20	36.53	36.53	25.84	0.95	0.10	0.05	20.0
WP-30	30.07	30.07	38.76	0.95	0.10	0.05	30.0
WP-40	23.61	23.61	51.68	0.95	0.10	0.05	40.0

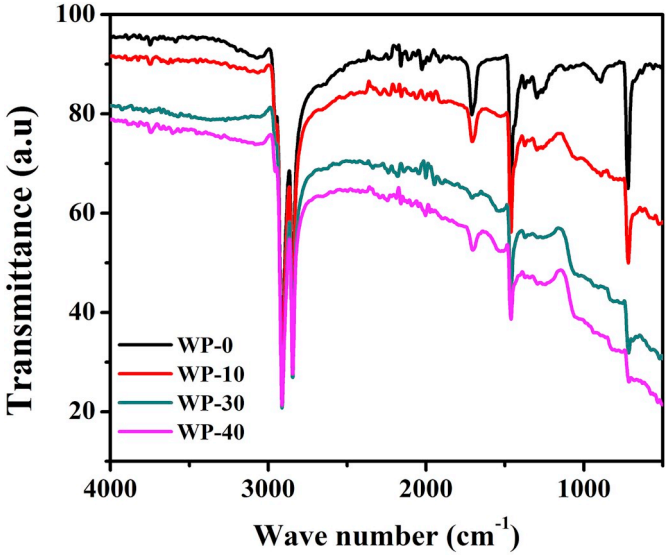

Fig. 4. Theoretical and experimental densities of HDPE/B_4C composites.

electron Rheodrive 4, Beverly USA) at 150 °C and 60 rpm for up to 10 min. The admixture was then hot pressed at 145 °C and 10 MPa load for 1 min (GIBITRE Instruments, Italy). It was then cold pressed to room temperature at 2 MPa load for 30 min to fabricate thin sheets (thickness, ~0.8 mm). For neutron shielding experiments, same procedure was followed to obtain a thick slab (thickness, ~25.4 mm). The resulted sheets/slabs were stored in self-sealing PE bags. Fig. 1 shows photographs of fabricated composite formulations.

Five distinct PE/B_4C composites were developed. Details of formulations are presented in Table 1. Stearic acid (1%) was used as a lubricant. Irganox-1076 (0.1%) and irgafos-168 (0.05%) were used as anti-oxidants in every formulation. All percentages are given by mass.

2.3. Characterizations

Density was measured by using a gas pycnometer (Micromeritics USA, model: AccuPyc-II 1340). Three distinct samples for every formulation were evaluated. Morphology of samples was determined by using scanning electron microscopy (SEM, JOEL USA, model: JSM-6490A). X-ray diffraction (XRD) analysis was performed using HR-XRD (Bruker AXS Germany, model: D8 Discover) with Cu-Kα radiation (λ = 1.540 A°, 2θ = 10°-50°). Thermal analysis was performed using simultaneous thermal analyzer (Mettler Toledo USA, model: TGA/DSC 1, STARe system) under nitrogen environment (flow rate = 50 mL min^{-1}, T = 49 °C–600 °C). Mechanical characterization was performed by using universal testing machine (SANS China) according to ASTM-D638 standard at a strain rate of 50 mm/min. At least five samples were tested for every formulation. Fast neutron shielding was measured against 1 Ci, Am-Be source (NCS-R.S USA).

2.3.1. Neutron shielding simulation

MCBEND® is a general purpose radiation transport code that can calculate charged particle, gamma ray, and neutron transport in subcritical systems. Moreover, different radiation types can also be coupled. Flexible geometry and modeling package are used in MCBEND® to model accurate transport of individual particles employing fine energy group representations. The code simulates what happens in practice, and performs a numerical experiment of the system under study. MCBEND® has versatile source description options and powerful automatic acceleration options for maximum productivity. Nuclear data libraries included in this code are UKNDL, JEFF, ENDF/B-VI and JENDL. The validation database covers many of the materials and geometries that are encountered in the nuclear industry and is subject to ongoing evaluation and improvement (Avery and Locke, 1992; Geoff et al., 2017; Khan et al., 2017).

Fig. 2 represents schematic diagram used for measuring neutron dose transmission through developed composites. The same setup was simulated in MCBEND® software. A solid-state neutron detector (ATOMTEX, Belarus) with He-3 probe (BDKN-01) was used for the measurement of neutron dose. Fig. 2 shows geometrical setup employed for the evaluation of neutron dose transmission. The MCBEND® code has been used for neutron transport calculation and estimation of the equivalent dose rate in 0.45 m distance from the Am-Be source. For this calculation, the source was considered as a pure neutron emitter with 1 Curie strength (4.6×10^6 neutrons/cm^3). In order to reduce the statistical errors, 50 million histories were considered in each simulation. Results showed a reasonable uncertainty confidence level. ENDF/B-VI library was referred for neutron cross section data.

3. Results and discussion

3.1. Density

Linear rule of mixture is a simple empirical method permitting to estimate properties of mixtures composed by two or more than two different materials with different nature. Upper bound and lower bound of density are calculated by using equations (1) and (2) respectively (Callister and Rethwisch, 2010);

$$\rho_c = w_r(\rho_r) + w_f(\rho_f) \quad (1)$$

$$\rho_c = \frac{100}{\left(\frac{w_r}{\rho_r} + \frac{w_f}{\rho_r}\right)} \quad (2)$$

Where, ρ_c, ρ_r, and ρ_f, are densities of composite formulation, PE matrix, and B_4C respectively. w_c, w_r, and w_f are weight fractions of composite, PE matrix, and B_4C respectively. Experimental density and theoretical density values are shown in Fig. 3. WP-10 is 8.69% heavier than that of neat PE matrix. On the other hand, WP-40 is 43.35% heavier as compared to the neat PE matrix. High density of WP-40 is ascribed to the presence of relatively dense B_4C (2.52 g cm^{-3}) filler in light PE (0.952 g cm^{-3}) matrix. Heavier B_4C occupies the inter-chain free space of PE matrix, thereby increasing the density of composite formulation without significantly increasing volume. This increase in density of PE matrix with the addition of B_4C may also result in an improvement in the crystallinity and stiffness of composite formulations.

3.2. Structural analysis

Fig. 4 shows the representative Fourier Transform Infrared (FTIR) spectra of neat polyethylene as well as its composites with B_4C. As it can be observed from the spectra, HDPE exhibited its characteristics bands at 2918 cm^{-1}, 2841 cm^{-1}, 1460 cm^{-1}, and 719 cm^{-1}, which are ascribed to the stretching and bending vibrations of PE (Fig. 4) (Gulmine et al., 2002; Shafiq and Yasin, 2012). The spectra of composites also exhibited similar peaks as observed in the PE. In addition, composites showed a new band at 1523 cm^{-1}, which is ascribed to the boron carbide (Fig. 4) (Wang et al., 2018). These results reveal that the

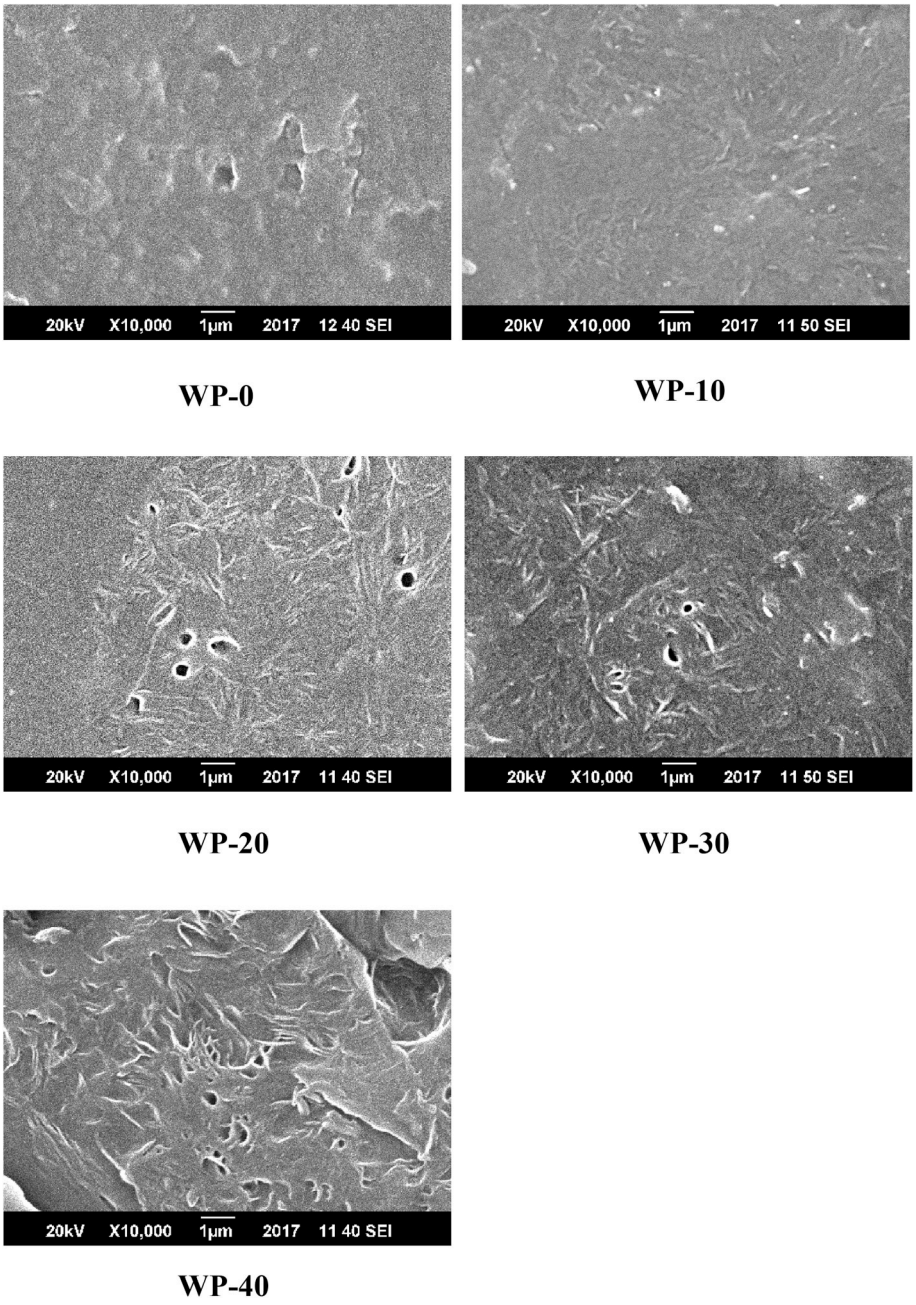

Fig. 5. SEM images of HDPE/B_4C composites.

chemical structure of neat HDPE remained unchanged with the addition of B_4C rendering it as a physical dispersion of the filler into the polymer matrix.

3.3. Morphological analysis

Crystalline polymer regions typically show rough and rugged surface morphology due to the presence of spherulites. PE is a semi-crystalline thermoplastic with varying degrees of amorphous and crystalline regions (Caminiti et al., 2000; Carraher, 2003; Sperling, 2006b). Fig. 5 shows SEM images of the surface of neat and borated composite formulations. The surface morphology of borated composites strongly depends on the content of boron. WP-0 shows uniform and continuous PE surface structure. WP-10 retains the uniform and continuous surface structure of WP-0. However, for WP-20, WP-30 and WP-40 composites, the surface morphology got rugged and rippled which might be due to the dispersion of B_4C filler into PE matrix. Moreover, this may also reflect as increase in the degree of crystallinity of composites.

3.4. X-ray diffraction

XRD was performed to investigate the structure of composites and extent of mixing of individual components of composites. Fig. 6 summarizes XRD spectra and percent crystallinity of all composite

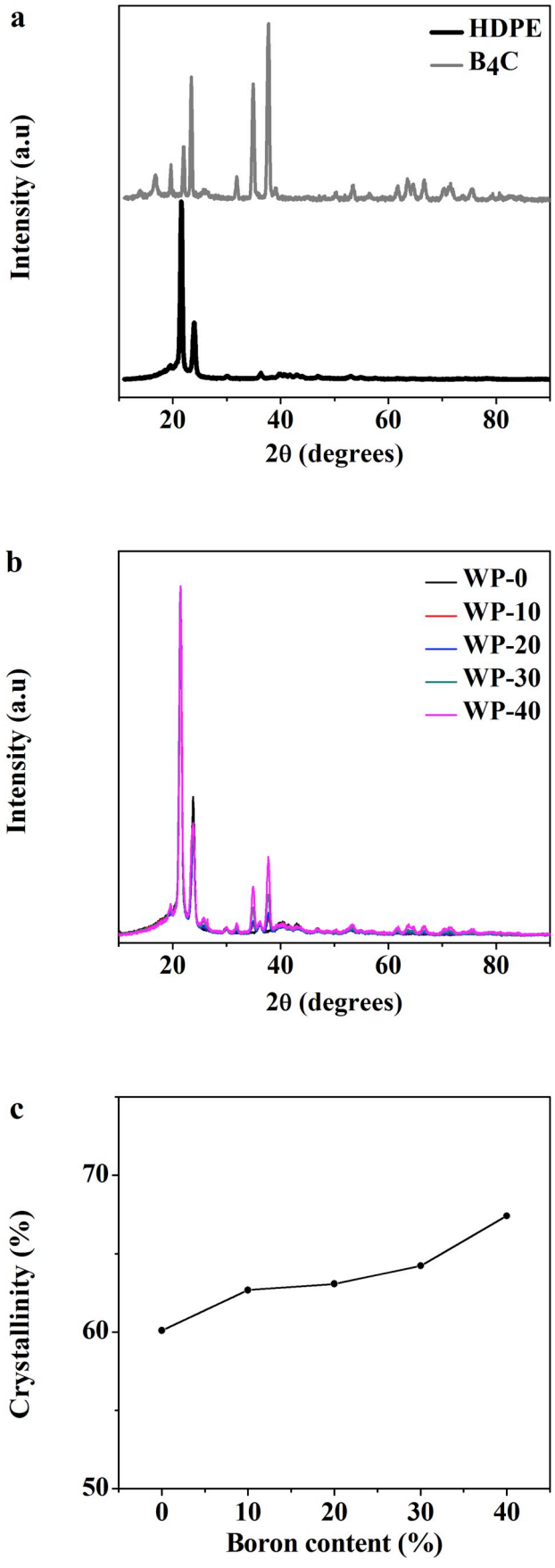

Fig. 6. XRD patterns and percent crystallinity of HDPE/B_4C composites.

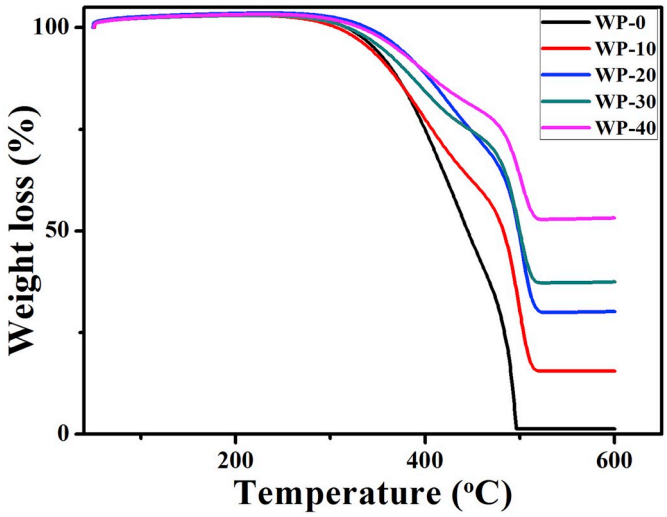

Fig. 7. Thermo-gram (TG) curves of HDPE/B_4C composites.

Table 2
Mechanical properties of HDPE/B_4C composites.

Formulation code	Elastic Modulus (MPa)	Strength at break (MPa)	Elongation at break (MPa)
WP-0	209.02 ± 3	10.90 ± 0.05	8.55 ± 0.53
WP-10	215.51 ± 22	9.63 ± 0.08	7.14 ± 0.94
WP-20	261.39 ± 31	11.27 ± 0.06	7.04 ± 0.74
WP-30	462.56 ± 21	7.20 ± 0.06	2.84 ± 0.08
WP-40	342.85 ± 21	7.24 ± 0.33	3.71 ± 0.39

formulations. The XRD spectrum of HDPE showed peaks with maximum intensity appeared at 2θ = 21.4° followed by a less intense peak at 2θ = 23.8°. Moreover, the amorphous content was represented by a broad hollow at 2θ = 20.8°, which indicated semi-crystalline nature of PE. The spectra of B_4C showed its characteristics peaks at 2θ = 16.8°, 19.8°, 22.1°, 23.5°, 31.8°, 34.9°, and 37.7°. Borated composites (WP10, WP20, WP30, and WP40) showed the characteristics peaks of PE as well as two additional peaks at 2θ = 34.9° and 37.7° indicating the existence/presence of B_4C filler into PE matrix as well as an improvement in the crystallinity in the composites.

Fig. 6-c represents percent crystallinity of composite formulations. Percent crystallinity was obtained by integrating peaks at 2θ = 20.88° (amorphous hollow), 21.46°, 23.82°, 34.9° and 37.7° (crystalline peaks) (Akishino et al., 2016). Addition of 40% of boron increased percent crystallinity of neat WP-0 formulation by 7.4%. This increase in percent crystallinity might be attributed to B_4C occupying less ordered and less dense amorphous regions of PE matrix. Ordered B_4C might have introduced its crystalline character to these amorphous regions which was depicted by extra intense peaks in borated formulations. Due to this increase in the percent crystallinity, borated composite formulations were denser and expected to be stiffer than that of neat composite formulation (Carraher, 2003).

3.5. Thermogravimetric analysis

Thermogravimetric analysis (TGA) provides a rapid method for the determination of thermal decomposition and reaction mass change of a material (Akay, 2006; Biron, 2013). Thermo-grams (TG) of all borated composite formulations are shown in Fig. 7, which show almost similar

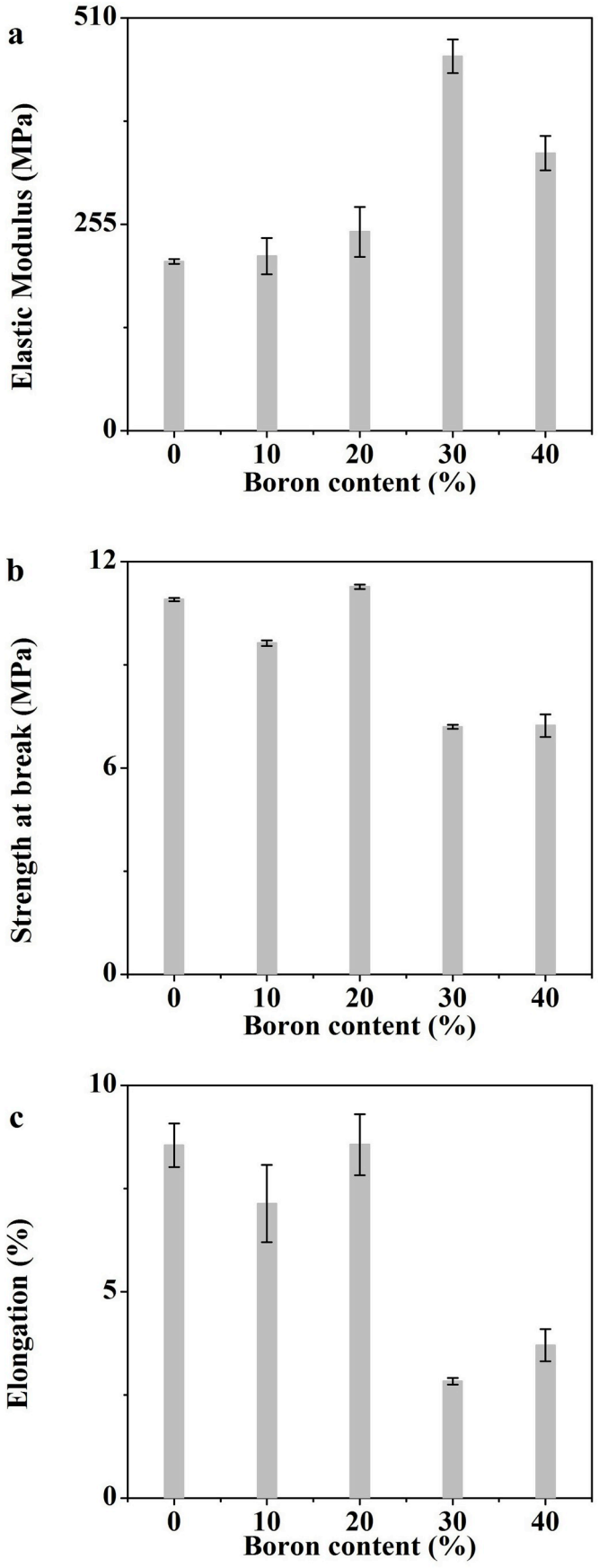

Fig. 8. Modulus of elasticity (a), Strength at break (b), and Elongation at break (c) of HDPE/B_4C composites.

Table 3
Density and mass fractions of HDPE/B_4C composites.

Formulation code	Density ($g.cm^{-3}$)	C (%)	H (%)	B (%)
WP-0	0.9285	85.37	14.61	0
WP-10	1.0348	77.15	12.72	10.1
WP-20	1.0900	68.91	10.83	20.22
WP-30	1.2044	60.67	8.94	30.33
WP-40	1.3647	52.44	7.05	40.45

behavior for up to 200 °C regardless of boron content. TGA curves of composite formulations show single step degradation profile, which indicate homogeneity and uniform distribution of B_4C in polymer matrix. The position of weight loss curves shifts towards higher temperature side with an increase in the boron content, which indicates an improvement in the thermal stability of composites with the addition of boron carbide. Therefore, the addition of B_4C increased the thermal stability of borated composite formulations.

3.6. Mechanical properties

Table 2 summarizes average values for tensile elastic modulus, strength at break, and elongation at break for different composite formulations. Fig. 8 shows the effect of increasing boron content on tensile elastic modulus, strength at break, and elongation at break values respectively. A gradual increase in the elastic modulus was observed with an increase in B_4C content. At high B_4C content, particle-particle interactions govern composite fracture mechanics. These interactions in turn influence modulus values which increase with an increase in the filler content (Harrison et al., 2008b). Structure-property relationship also dictates that, increase in filler content provides resistance to crack propagation (Carraher, 2003). This trend was obvious in Fig. 8(c). However, in WP-40, a slight decrease in elastic modulus was observed. Here, brittle B_4C has gained almost half of relatively ductile matrix. Fracture mechanics was now governed by brittle B_4C which allows less deformation in the elastic region (Shin et al., 2014).

On the other hand, decrease in the strength at break and elongation at break was observed with increase in B_4C content as shown in Fig. 8(b) and (c) respectively. This phenomenon can be explained by filler-matrix de-bonding theory (Biron, 2013; Sperling, 2006a; Yasin and Khan, 2008). Polymer matrix de-bonds from B_4C particles when adhesive forces at interface are overcome by applied tensile stress. Debonded B_4C particles act as stress raisers (holes in matrix) in resin ligaments leading to its yielding. Number of stress raiser holes is directly proportional to B_4C content. This results in sequential decrease in yield strength and elongation with volumetric increase in B_4C.

3.7. Neutron shielding measurements

Neutron shielding mainly involves absorption of high energy neutrons. The process requires hydrogenous material for moderating fast neutrons for subsequent absorption by shielding material. High hydrogen content is desirable for moderating fast neutrons through elastic scattering to effectively reduce the neutron energy down towards lower-energy regions i.e. slow neutrons (Ancharova et al., 2017; Granada et al., 1987; Harrison et al., 2008b; Sundar et al., 1996).

The measurement of fast neutron shielding relies on effective removal cross sections (Σ_r). Effective removal cross-section is a measure of the probability that fast or fission energy neutrons undergo a first collision, which removes them from the group of the penetrative uncollided neutrons. This effective cross section is often applicable to thick sections with multiple elements mixed together. The dose rate for a neutron beam transmitted through mass thickness is represented by

Table 4
Neutron shielding properties of HDPE/B_4C composites.

Boron (%)	Mass removal cross section ($cm^2.g^{-1}$)		Relative difference (%)	HVL (cm)	
	Experimental data	MCBEND® data		Experimental data	MCBEND® data
0	0.0960 ± 0.0045	0.1071 ± 0.0003	10.50	7.22 ± 0.34	6.47 ± 0.02
10	0.0948 ± 0.0059	0.0961 ± 0.0008	1.31	7.31 ± 0.45	7.21 ± 0.06
20	0.0864 ± 0.0050	0.0828 ± 0.0005	2.66	8.02 ± 0.46	8.37 ± 0.05
30	0.0678 ± 0.0037	0.0593 ± 0.0002	14.43	10.22 ± 0.56	11.69 ± 0.04
40	0.0523 ± 0.0038	0.0577 ± 0.0005	8.64	13.25 ± 0.96	12.01 ± 0.10

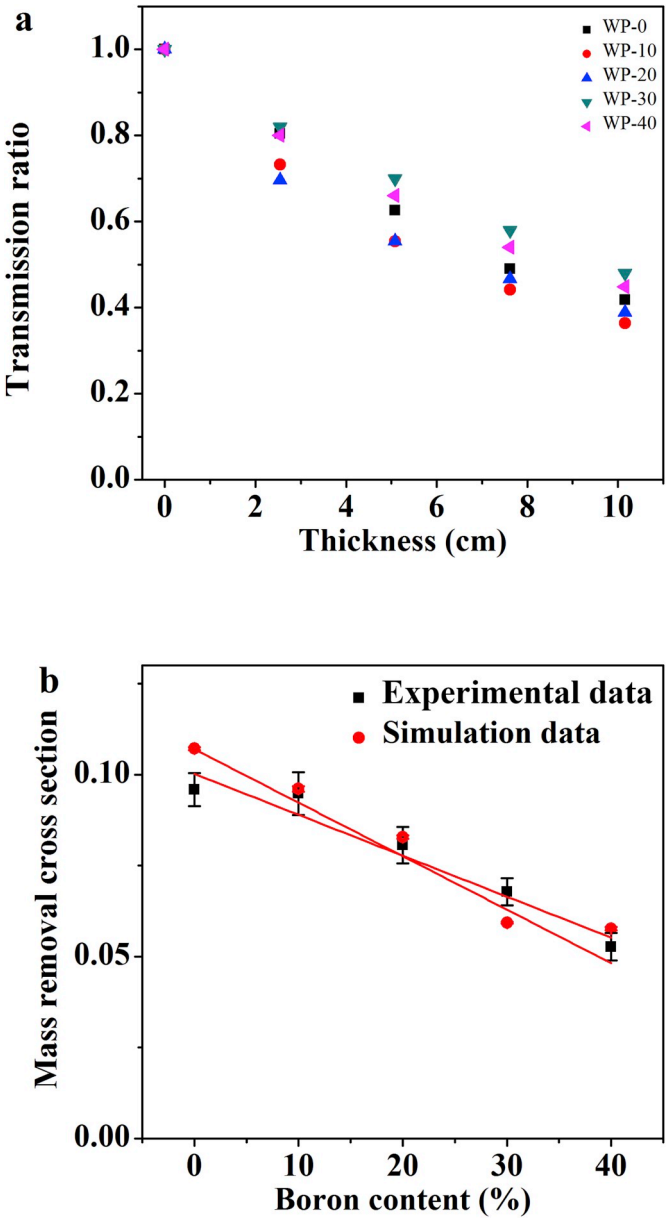

Fig. 9. Dose transmission data (a) and mass removal cross section (b) of HDPE/B_4C composites.

equation (4);

$$\Sigma_r = \frac{\ln\left(\frac{R_x}{R_o}\right)}{x} \quad (4)$$

where, R_x is the dose rate when shield of thickness x (units) is present between source and detector, R_o is the dose rate when no shield of thickness x (units) is present between source and detector. Transmission ratio is simply a ratio between dose rates with and without composite shield respectively. Half value layer (HVL) of composite formulations can be calculated using equation (5) (Zhang et al., 2017).

$$HVL = \frac{\ln(2)}{\Sigma_r} \quad (5)$$

Table 3 presents the density and weight fractions of different constituents of HDPE/B_4C composites used in both experimental and MCBEND® simulated neutron shielding measurements. Table 4 summarizes the mass removal cross section data of both experimental and MCBEND® simulated neutron shielding measurements. Fig. 9 represents neutron dose rate data and mass removal cross section. Relative difference between experimental data and MCBEND® simulated data is not more than 15%. From Table 3, it appeared that for every 10% increase in boron content, there is a consequent decrease of 1.89% in hydrogen content. Moreover hydrogen content dropped 5.6% from WP-10 to WP-40. Since hydrogen both scatters and thermalize fast neutrons, it optimal weight fraction of both boron and hydrogen is necessary for better shielding properties (Abd and Elkady, 2014; Elmahroug et al., 2014; Harrison et al., 2008a; Shin et al., 2014).

For this study, WP-10 showed an effective balance between boron and hydrogen to achieve highest mass removal cross section and half value layer (HVL) at the given experimental and simulation parameters. For WP-10, fast neutron shielding increased by ~40% than WP-40 on equivalent density basis. Therefore, WP-10 is the best fast neutron shielding material among all HDPE/B_4C developed for this study. Moreover, WP-10 is ~1.5 times lighter than WP-40.

Table 5 shows a brief comparison of this study with the previous research work. Abd Elwahab et al., 2019 developed HDPE/borax sand/cement composite pastes with varying weight percentages of boron. Samples were evaluated for neutron and gamma shielding. The removal cross section values for the composites containing 1.24% and 7.72% boron were found to be 0.1000 cm^{-1} and 0.1570 cm^{-1}, respectively. However, these composites were considerably heavier than that of the WP-10 composite as fabricated in this study (B content 1.24%, 17% heavier than that of WP-10; B content 7.72%, 50% heavier than that of WP-10). Moreover, WP-10 composite possessed better mass removal cross section. Similarly, other researchers have theoretically calculated the fast neutron removal cross sections of neat PE as well as its hybrids containing 1.0% and 8.97% of boron (Table 5) (Abd and Elkady, 2014; El-Khayatt, 2010; Elmahroug et al., 2014). In our study, the removal cross sections are obtained both by MCBEND® simulation and experimental measurements. WP-10 showed reasonable mass removal cross-section as well as exhibited less density than that of the composites developed in the previous studies; thus making it a suitable candidate for neutron shielding. Similarly, the values obtained from the simulation were in close agreement with the experimental values.

4. Conclusions

In this study, PE composites with high boron content were investigated for fast neutron shielding against Am-Be neutron source. All borated composites were denser, more crystalline, mechanically stiffer,

Table 5
Comparison of borated polymer composites for fast neutron shielding applications.

Sr. No.	Composition	B(%)	ρ (g.cm^{-3})	TS (MPa)	Σ_r (cm^{-1})	Σ_r/ρ(cm^2.g^{-1})	Ref
1.	HDPE	0	0.9285	10.90	0.0891	0.0960	Current study
	HDPE + B	10.0	1.0348	9.63	0.0981	0.0948	
2.	HDPE + Borax	1.24	1.78	n.d	0.1000	0.0562	(Abd Elwahab et al., 2019)
		7.72	2.08	n.d	0.1570	0.0754	
3.	PE	0	0.9200	n.d	0.1186	0.1289	(El-Khayatt, 2010)
	PE + B	1.0	1.700	n.d	0.1221	0.0718	
	PE + B	8.97	1.600	n.d	0.0953	0.0596	
4.	PE	0	0.9200	n.d	0.1870	0.2032	(Elmahroug et al., 2014; Abd and Elkady, 2014)
	PE + B	1.0	1.700	n.d	0.1182	0.0738	
	PE + B	8.97	1.600	n.d	0.0926	0.0578	

ρ, density; TS, tensile strength; $\boldsymbol{\Sigma_r}$, removal crosssection; and $\boldsymbol{\Sigma_r}$/ρ, mass removal cross-section; n.d, not determined.

and thermally more stable than that of neat composite formulation. These enhancements in physico-chemical properties can be attributed to higher boron content in borated formulations than neat PE. Composite formulation containing 10% of boron content reduced fast neutron dose rate by 63.6% and achieved highest mass removal cross section due to optimal balance of hydrogen and boron contents. Moreover, WP-10 is superior to all borated composite formulations developed for this study w.r.t. neutron shielding, mechanical durability, thermal stability, weight and density. Owing to these attributes, it may be worthy for fast neutron shielding applications in the range of neutron energies of ~4.5 MeV.

Appendix A. Supplementary data

Supplementary data to this article can be found online at https://doi.org/10.1016/j.radphyschem.2019.108450.

References

Abd, A.A.El, Elkady, A.S., 2014. A method for simultaneous determination of effective removal cross-section for fast neutrons and mass absorption coefficient for gamma rays. SOJ Mater. Sci. Eng. 6–11.

Abd Elwahab, N.R., Helal, N., Mohamed, T., Shahin, F., Ali, F.M., 2019. New shielding composite paste for mixed fields of fast neutrons and gamma rays. Mater. Chem. Phys. 233, 249–253. https://doi.org/10.1016/j.matchemphys.2019.05.059.

Akay, M., 2006. An Introduction to polymer-matrix composites. Headway. https://doi.org/10.1017/CBO9780511623806.

Akishino, J.K., Cerqueira, D.P., Silva, G.C., Swinka-Filho, V., Munaro, M., 2016. Morphological and thermal evaluation of blends of polyethylene wax and paraffin. Thermochim. Acta 626, 9–12. https://doi.org/10.1016/j.tca.2016.01.002.

Ancharova, U.V., Mikkhailenko, M.A., Sharafutdinov, M.R., Tolochko, B.P., Gerasimov, K.B., Korobeynikov, M.V., Bryazgin, A.A., 2017. Structure and properties of radiation modified polyethylene. In: XII International Conference Radiation-Thermal Effects and Processes in Inorganic Materials, . https://doi.org/10.1088/1757-899X/168/1/012110.

Avery, A.F., Locke, M., 1992. NEACRP Comparision of Codes for the Radiation Protection Assessment of Transportation Packages.

Aygün, B., Budak, G., 2012. A new neutron absorber material : oil loaded paraffin wax. Nucl. Sci. Technol. 661, 33–39.

Biron, M., 2013. Thermoplastics and Thermoplastics Composites. Elsevier Ltd, Oxford, UK. https://doi.org/10.1016/B978-1-4557-7898-0.00002-0.

Callister, W.D., Rethwisch, D.G., 2010. Materials Science and Engineering: an Introduction, Materials Science and Engineering an Introduction. John Wiley & Sons, Hoboken, New Jersey. https://doi.org/10.1016/0261-3069(91)90101-9.

Caminiti, R., Pandolfi, L., Ballirano, P., 2000. Structure of polyethylene from X-ray powder diffraction: influence of the amorphous fraction on data analysis. J. Macromol. Sci. Phys. 39, 37–41. https://doi.org/10.1081/MB-100100400.

Carraher, C., 2003. Polymer Chemistry, sixth ed. Marcel Dekker, Inc., New York Polymer Chemistry. https://doi.org/10.1039/c4py01415d.

El-Khayatt, A.M., 2010. Calculation of fast neutron removal cross-sections for some compounds and materials. Ann. Nucl. Energy 37, 218–222. https://doi.org/10.1016/j.anucene.2009.10.022.

Elmahroug, Y., Tellili, B., Souga, C., 2014. Determination of shielding parameters for different types of resins. Ann. Nucl. Energy 63, 619–623. https://doi.org/10.1016/j.anucene.2013.09.007.

Geoff, D., Adam, B., Brendan, T., Paul, S., 2017. Using MCBEND for neutron or gamma-ray deterministic calculations. In: EPJ Web of Conferences, pp. 1–6. https://doi.org/10.1051/epjconf/201715306032.

Granada, J.R., Dawidowski, J., Mayer, R.E., Gillette, V.H., 1987. Thermal neutron cross section and transport properties of polyethylene. Nucl. Instrum. Methods Phys. Res. A 261, 573–578. https://doi.org/10.1016/0168-9002(87)90370-6.

Groves, K., 2017. Simple experimental design for calculation of neutron removal cross sections. McMaster J. Eng. Phys. 1–5.

Gulmine, J.V., Janissek, P.R., Heise, H.M., Akcelrud, L., 2002. Polyethylene characterization by FTIR. Polym. Test. 21, 557–563. https://doi.org/10.1016/S0142-9418(01)00124-6.

Harrison, C., Burgett, E., Hertel, N., Gmlke, E., 2008a. Polyethylene/boron composites for radiation shielding applications. Composites 484–491. https://doi.org/10.1002/App.27949.

Harrison, C., Weaver, S., Bertelsen, C., Burgett, E., Hertel, N., Grulke, E., 2008b. Polyethylene/boron nitride composites for space radiation shielding. J. Appl. Polym. Sci. 109, 2529–2538. https://doi.org/10.1002/app.27949.

John, R., Lamarsh, A.J.B., 1955. Introduction to Nuclear Engineering, American Journal of Physics. Prentice Hall, Upper Saddle river, New Jersey. https://doi.org/10.1119/1.1933896.

Khan, R., Naveed Khan, M., A Qureshi, M., 2017. Benchmarking of MCBEND Computer Code against the PWR Shield Design. pp. 127–129 IEEE.

Kyrieleis, A., 2014. Monte Carlo Simulation of Nuclear Reactions.

Martin, J.E., 2013. Physics for Radiation Protection. Wiey-VCH, Weinheim,Germany.

Murray, R.L., 2014. An Introduction to the Concepts, Systems, and Applications of Nuclear Processes. Butterworth Heinemann, Raleigh, North Carolina.

Shackelford, J.F., Alexander, W., 2000. CRC Materials Science and Engineering Handbook, third ed. Crc Handbook. https://doi.org/10.1201/9781420038408.

Shafiq, M., Yasin, T., 2012. Effect of gamma irradiation on linear low density polyethylene/magnesium hydroxide/sepiolite composite. Radiat. Phys. Chem. 81, 52–56. https://doi.org/10.1016/j.radphyschem.2011.09.009.

Shin, J.W., Lee, J.W., Yu, S., Baek, B.K., Hong, J.P., Seo, Y., Kim, W.N., Hong, S.M., Koo, C.M., 2014. Polyethylene/boron-containing composites for radiation shielding. Thermochim. Acta 585, 5–9. https://doi.org/10.1016/j.tca.2014.03.039.

Sperling, L.H., 2006a. Introduction to physical polymer science. In: Journal of Chemical Education, fourth ed. John Wiley & Sons, Hoboken New Jersey. https://doi.org/10.1021/ed078p1469.1.

Sperling, L.H., 2006b. Introduction to Physical Polymer Science, Fourth. John Wiley & Sons, Pennsylvania. https://doi.org/10.1021/ed078p1469.1.

Sundar, K.L., Radhakrishnan, G., Reddi, B.R., 1996. Borated polymer composite for fast neutron shielding (Americium-Beryllium source). Polym. Plast. Technol. Eng. 35, 561–566. https://doi.org/10.1080/03602559608000592.

Uhlář, R., Alexa, P., Pištora, J., 2013. A system of materials composition and geometry arrangement for fast neutron beam thermalization: an MCNP study. Nucl. Instrum. Methods Phys. Res. Sect. B Beam Interact. Mater. Atoms 298, 81–85. https://doi.org/10.1016/j.nimb.2013.01.032.

Wang, J., He, Y., Xie, Z., Chen, C., Yang, Q., Zhang, C., Wang, B., Zhan, Y., Zhao, T., 2018. Functionalized boron carbide for enhancement of anticorrosion performance of epoxy resin. Polym. Adv. Technol. 29, 758–766. https://doi.org/10.1002/pat.4181.

Yasin, T., Khan, M.N., 2008. High density polyethylene/boron carbide composites for neutron shielding. E-Polymers. https://doi.org/10.1515/epoly.2008.8.1.670.

Zhang, Xianlong, Yang, M., Zhang, Xiaomeng, Wu, H., Guo, S., Wang, Y., 2017. Enhancing the neutron shielding ability of polyethylene composites with an alternating multi-layered structure. Compos. Sci. Technol. 150, 16–23. https://doi.org/10.1016/j.compscitech.2017.06.007.